



# Kahramanmaraş Sutcu Imam University

## Journal of Engineering Sciences



Geliş Tarihi : 26.11.2023  
Kabul Tarihi : 29.04.2024

Received Date : 26.11.2023  
Accepted Date : 29.04.2024

### IMPACT OF ELECTRIC CARS ON THE CRASH PERFORMANCE OF LONGITUDINAL BARRIERS

### ELEKTRİKLİ ARAÇLARIN GÜVENLİK BARIYERLERİNİN ÇARPIŞMA PERFORMANSINA ETKİSİ

Ayhan Öner YÜCEL<sup>1\*</sup> (ORCID: 0000-0001-5888-2809)

<sup>1</sup> Aydın Adnan Menderes University, Department of Civil Engineering, Aydın, Türkiye

\*Sorumlu Yazar / Corresponding Author: Ayhan Öner YÜCEL, aoyucel@adu.edu.tr

#### ABSTRACT

The use of battery electric vehicles (EVs) is spreading around the world due to their advantages. The presence of large batteries makes electric cars heavier, and due to their position, the vehicle's center of gravity is lowered compared to conventional internal combustion engine cars. The weight of an impacting vehicle is one of the critical parameters for the acceptable performance of longitudinal barriers. It is anticipated that EVs could pose failure risks for conventional safety hardware, yet there is still no revision regarding the use of EVs in existing full-scale crash test standards. In this study, the effect of electric cars on the crash performance of the H1 containment level longitudinal steel safety barrier was investigated through computer simulations. Three different vehicle models, each weighing 900 kg and currently used for TB11 finite element analyses, were modified according to the features of the selected reference EVs. Barrier crash performance was evaluated in terms of occupant safety and structural adequacy. Analysis results showed that with increasing vehicle weights in EV tests, injury severity indices become smaller, while the damage to the barrier gets larger. Further investigation of the crash performance of existing barriers with EVs is highly recommended.

**Keywords:** Electric car, crash test, steel barrier, finite element analysis, roadside safety

#### ÖZET

Elektrikli araçların kullanımı, avantajları nedeniyle tüm dünyada yaygınlaşmaktadır. Büyük bataryalar elektrikli arabaları ağırlaştırmakta ve konumları nedeniyle aracın ağırlık merkezini, geleneksel içten yanmalı motorlu arabalara göre daha alçak hale getirmektedir. Çarpma aracın ağırlığı, güvenlik bariyerlerinin kabul edilebilir performansı için önemli parametrelerden biridir. Elektrikli araçların geleneksel güvenlik tertibatları için başarısızlık riski oluşturabileceği öngörülmektedir. Ancak mevcut tam ölçekli çarpışma testi standartlarında elektrikli araçların kullanımına dair henüz bir güncelleme bulunmamaktadır. Bu çalışmada, elektrikli arabaların H1 performans seviyesi çelik güvenlik bariyerinin çarpışma performansına etkisi bilgisayar simülasyonlarıyla incelenmiştir. Her biri 900 kg ağırlığında olan ve halihazırda TB11 sonlu elemanlar analizlerinde kullanılan üç farklı araç modeli, seçilen referans elektrikli araçların özelliklerine göre modifiye edilmiştir. Bariyerin çarpışma performansı, yolcu güvenliği ve yapısal yeterlilik açısından değerlendirilmiştir. Analiz sonuçları, elektrikli araç testlerinde araç ağırlığının artmasıyla yaralanma şiddet indekslerinin küçüldüğünü, bariyerdeki hasarın ise büyüdüğünü göstermiştir. Mevcut bariyerlerin elektrikli araçlarla çarpışma performansına ilişkin daha fazla araştırma yapılması önerilmektedir.

**Anahtar Kelimeler:** Elektrikli araç, çarpışma testi, çelik bariyer, sonlu elemanlar analizi, yol kenarı güvenliği

## INTRODUCTION

Longitudinal barriers, positioned passively along the roadside and running parallel to the road, are safety systems designed to prevent vehicles from veering off the road in case of an accident. These road safety barriers must meet specific evaluation criteria related to material design, installation, and testing. Typically, the road safety barrier systems used on European highways must adhere to the specifications defined in the European standard EN 1317 (EN 1317-2, 2010). This standard outlines the procedures for testing and certifying newly developed guardrails, providing detailed crash test specifications that include vehicle containment levels, vehicle categories, impact velocities, and impact angles. Additionally, it specifies vehicle characteristics, such as type, dimensions, mass, and mass distribution.

All vehicles categorized in EN 1317 include those with conventional internal combustion engines (EN 1317-1, 2010). Similarly, the American MASH standard, which deals with the evaluation of road restraint systems, also lacks details on testing barriers with electric vehicles (EVs) (AASHTO, 2016). However, the use of electric vehicles has been steadily increasing in recent years (IEA, 2023). The presence of electric batteries in EVs results in a higher mass and a lower center of gravity compared to similarly sized gasoline or diesel cars. The crash performance of longitudinal barriers relies on various factors, such as the weight of the vehicle, impact speed, and the angle of impact (He & Lin, 2018). Given that weight is a crucial factor, there is concern that much heavier electric vehicles could pose a higher risk compared to gasoline or diesel cars of similar size. So far, there have been no established specifications regarding longitudinal barrier tests with electric cars. Therefore, there is a need to investigate the effects of electric cars on the performance of longitudinal safety barriers. Research on barrier crash tests considering the increased weight and lower center of gravity of electric cars could be incorporated into the upcoming revision of the European standard EN 1317.

Longitudinal barriers are divided into three main categories depending on their deformation characteristics (Kim et al., 2016). In terms of lateral deformation performance, concrete barriers are considered rigid, steel barriers are classified as semi-rigid, and cable barriers are representative examples of flexible barriers (Ozcanan & Atahan, 2021). The evaluation standards for guardrails employ a dual assessment approach: The first aspect focuses on the barrier's ability to ensure the safety of drivers and passengers, while the second aspect evaluates the structural adequacy of the barrier. Comprehensive testing is necessary before implementing designed roadside safety barriers to evaluate their safety and structural performance. The injury risk to occupants is assessed using two indices: the acceleration severity index (ASI) and the theoretical head impact velocity (THIV). Systems that pass these tests successfully receive certification and approval for implementation. The geometric features of barriers significantly affect performance (Molan et al., 2019; Molan & Ksaibati, 2021). Barrier height and post spacing are critical parameters for the safety performance of barriers (Teng et al., 2016). The severity of impact is significantly influenced by both the type and material of the post (Atahan & Yücel, 2013; Teng et al., 2016). In addition to barrier features, vehicle properties also affect the crash performance of the barrier. Even with the same weight, changes in vehicle geometric features could alter barrier crash performance (Atahan et al., 2013, 2014; Özcanan & Özcan, 2022). Therefore, there is a need to investigate the effects of increasingly used high-weight and low-center-of-gravity electric cars on the performance of existing barriers.

The use of Finite Element (FE) analysis in roadside safety assessments is indispensable due to the high costs and time constraints associated with conducting full-scale tests for developed systems. FE analysis offers significant advantages by enabling the creation of full-scale models that simulate real crash tests, and the results obtained align consistently with those from actual tests. This flexibility allows for an unlimited number of analyses using FE, facilitating the exploration of various parameters and variables. Numerous studies have investigated the crash performance of road safety systems by creating FE models (Langseth et al., 1999; Pawlak, 2016; Yücel et al., 2018; Gheres & Scurtu, 2022; Wolny et al., 2022). Comparisons between real crash tests and FE models have indicated that the computational models well represent actual conditions. Instead of conducting numerous expensive and labor-intensive real crash tests, FE simulations can be employed (Ren & Vesenjaj, 2005). The good agreement between simulation results and real crash tests enables the utilization of FE models during the development and certification process of guardrails (Borovinšek et al., 2007). In a recent study, the crash performance of Automated Driving Systems (ADS) when colliding with roadside hardware was investigated and compared to traditional vehicles (Reichert et al., 2020). The study employed various roadside hardware, different types of ADS, and impact configurations for finite element simulation using LS-DYNA software. In previous studies, the LS-DYNA program

was observed to be used for finite element analysis of the performance of roadside safety systems. In this study, the LS-DYNA software was employed (LSTC, 2012).

The main objective of this study is to investigate the impact of electric cars on the crash performance of existing longitudinal safety barriers. Crash analyses were conducted using 3-dimensional dynamic FE analysis software, LS-DYNA. For this investigation, an H1 containment level steel longitudinal barrier was employed. The FE model was validated by comparing the results of a real full-scale crash test and computer simulation of the TB11 test for the H1 barrier. To assess the effects of electric cars with a lower center of gravity and higher weight, three different car models were used in the FE simulations. Crash analyses of the H1 barrier were performed using the FE models of 900 kg weight cars and modified vehicle FE models based on selected reference electric cars. Finally, the impacts of electric cars on the severity of the collision were evaluated using ASI and THIV parameters, while the structural performance was assessed through working width (W) and the final condition of the test barrier.

## MATERIAL AND METHOD

### *Crash Performance Evaluation of Longitudinal Barriers according to EN 1317*

EN 1317 is the main standard that defines testing and certification procedures for roadside safety barriers. Road restraint systems employed on European highways must adhere to the specifications outlined in the European standard EN 1317 (EN 1317-2, 2010). The standard consists of eight separate parts. Terminology and general test criteria, including vehicle geometric details, are presented in EN 1317-1 (EN 1317-1, 2010). The second part (EN 1317-2, 2010) outlines test methods for longitudinal barriers, crash test acceptance criteria, and performance classes of the guardrails. This standard defines containment levels of safety barriers (low angle, normal, higher, and very high) and requires crash tests for each level. A total of 11 different crash tests are defined in the EN 1317-2. The standard provides vehicle type, impact speed, impact angle, and vehicle mass for each test. In this study, an H1 containment level safety barrier, classified as higher containment, was used to perform computer simulation crash tests. Table 1 presents the required crash tests for the H1 containment level and the details of those tests. As indicated in the table, an H1 safety barrier must undergo the TB11 and TB42 tests. For the acceptance of the barrier design, test results should meet the evaluation criteria described in EN 1317. In the TB11 test, a 900 kg car impacts an H1 barrier at a speed of 100 km/h at an angle of 20°. In the TB42 test, a 10000 kg rigid Heavy Goods Vehicle (HGV) impacts an H1 barrier at a speed of 70 km/h and an angle of 15°.

**Table 1.** The Details of Tests Required for H1 Containment Level (EN 1317-2, 2010)

Containment level	Required Test	Speed (km/h)	Angle (°)	Mass (kg)	Type of vehicle
Higher containment	TB11	100	20	900	Car
	TB42	70	15	10000	Rigid HGV

Crash test results of longitudinal barriers should meet the conditions outlined in EN 1317-2. Evaluation criteria can be classified into three main groups: structural adequacy, occupant risk, and vehicle trajectory. The most important conditions for crash test acceptance can be summarized as follows: the vehicle must not roll over during or after the test, barrier parts must not penetrate inside the occupant compartment, there must be no complete breakage in the longitudinal elements forming the barrier, and the vehicle must remain at the traffic side of installation (EN 1317-2, 2010). In this study, the impacts of electric cars on barrier performance were investigated. Therefore, the focus was solely on TB11 testing since this test deals with the testing of small passenger cars. One of the main purposes of the TB11 test is to evaluate the injury risk of occupants in the vehicle. ASI and THIV indices are used to assess the severity of injury (EN 1317-2, 2010). The ASI represents the impact intensity, while THIV quantifies the speed at which the occupant impacts with an object in the car during the collision. Accelerations in the x, y, and z directions are utilized to calculate ASI, as given in Equation (1).

$$ASI(t) = \sqrt{\left[\left(\frac{a_x}{\hat{a}_x}\right)^2 + \left(\frac{a_y}{\hat{a}_y}\right)^2 + \left(\frac{a_z}{\hat{a}_z}\right)^2\right]} \quad (1)$$

where,  $a_x$ ,  $a_y$ , and  $a_z$  represent the components of vehicle acceleration (measured in g, where g is gravitational acceleration) in the three axes.  $\hat{a}_x$ ,  $\hat{a}_y$ , and  $\hat{a}_z$  denote the threshold accelerations in the longitudinal (x), lateral (y), and

vertical (z) directions, respectively. These threshold values are specified in the standard as 12 g, 9 g, and 10 g, respectively. The ASI value obtained from this equation is expressed by Equation (2).

$$ASI = \max[ASI(t)] \tag{2}$$

The THIV value is calculated using the occupant's head speed inside the vehicle, as specified in Equation (3).

$$THIV = [V_{head\ x}^2(T) + V_{head\ y}^2(T)]^{0.5} \tag{3}$$

where  $V_{head\ x}$  and  $V_{head\ y}$  refer to the head velocity measurements in the longitudinal and lateral directions.  $T$  represents the time of flight required for theoretical head displacement equal to 600 mm in the x direction or 300 mm in the y direction.

Table 2 provides ASI ranges and their corresponding impact severity levels. The standard establishes the maximum acceptable THIV level as 33 km/h, with lower ASI values being desired for the safety of occupants.

**Table 2.** Impact Severity Levels According to EN 1317-2 (EN 1317-2, 2010)

Impact severity level	Characteristic values		
A	ASI ≤ 1.0		
B	1.0 < ASI ≤ 1.4	and	THIV < 33 km/h
C	1.4 < ASI ≤ 1.9		

The structural adequacy of barriers is critical for their acceptance. During a collision, permanent damage and deformations occur in the guardrail components. The amount of lateral movement is defined as working width (W) in the EN 1317 standard. The lateral deformation of the system depends on the rigidity of the barrier components and connection properties. Working width is determined by measuring the maximum lateral distance between the front side of the barrier facing traffic before the impact test and any part of the barrier during the collision. Table 3 provides working width (W) ranges and their corresponding classes. After the TB11 crash test, ASI, THIV, and W classes are reported along with other details.

**Table 3.** Working width classes (EN 1317-2, 2010)

Class	W1	W2	W3	W4	W5	W6	W7	W8
Working width (m)	W ≤ 0.6	W ≤ 0.8	W ≤ 1.0	W ≤ 1.3	W ≤ 1.7	W ≤ 2.1	W ≤ 2.5	W ≤ 3.5

### ***Details of H1 Containment Level Longitudinal Barrier Studied***

This study investigates the impacts of heavier and lower center of gravity electric cars on barrier performance, using the H1 containment level longitudinal steel barrier. This barrier system comprises two main components: C-type post and B-type rail. Additionally, bolts are used to connect the rails and to attach rails to the posts. In this system, the spacing between posts is 2 meters. The total height of the system from the ground to the top of the rail is 750 mm, with the posts embedded 750 mm into the soil. The post and rail thicknesses are 4 mm and 2.5 mm, respectively. The length of the B-type rail is 4320 mm. The dimensions of the longitudinal barrier system components and their other details are provided in Figure 1. These drawings pertain to the system used for the TB11 crash test performed at an accredited test center located in Italy (CSI, 2014).

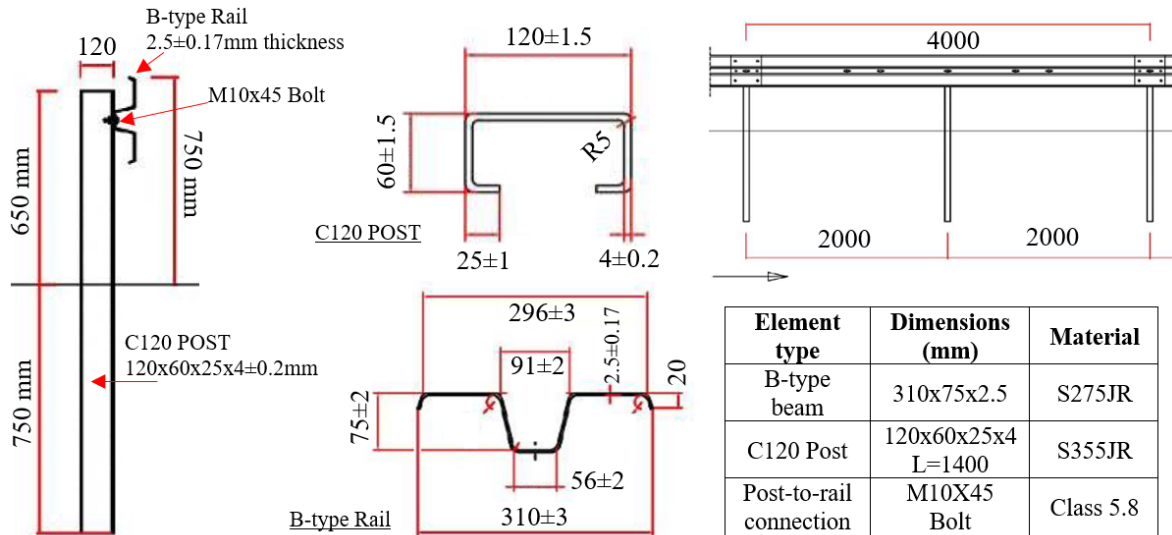


**Figure 1.** Details of H1 Containment Level Barrier Used in This Study (CSI, 2014)

To assess the crash performance of this barrier, its finite element (FE) model was created. The FE model of the H1 barrier system is depicted in Figure 2. In the FE model creation step, material models and geometries of the barrier components were defined to accurately represent the actual case. A three-dimensional, large deformation finite element code, LS-DYNA, was employed to conduct the crash analyses (LSTC, 2012). In the LS-DYNA model, rail and post parts were modelled as shell elements. To define steel material properties, the MAT024 (piecewise linear plasticity) material model was used in LS-DYNA. For simulating bolt connections between the rail and post, beam elements with failure were defined. The properties of the bolt were defined using the MAT098 (simplified Johnson Cook) material model. The soil was also modelled to simulate the post-soil interaction more accurately during the collision. For the solid soil parts, the MAT193 (Drucker Prager) material model was utilized.

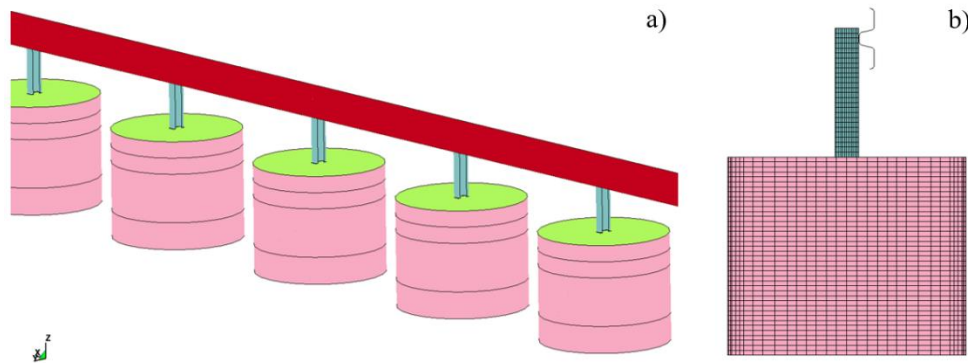


**Figure 2.** Finite Element Model of H1 Barrier System: **a)** General View, **b)** Side View (mesh view is on)

### Validation of Finite Element (FE) Model

The accuracy of the barrier FE model needs validation through an actual crash test according to EN 1317. Safety and performance parameters obtained from actual crash tests and computer simulation results should be close enough to satisfy error tolerances in EN 16303 (BS EN 16303:2020, 2020). After this validation, the developed model could be used for further crash simulations. Actual crash test data for the TB11 test were available. Therefore, a full-scale FE model of the H1 system for TB11 test conditions was developed using LS-DYNA. In the validation phase of the study, a 900 kg car FE model developed and validated by the National Crash Analysis Center was used (NCAC, 2008). The barrier model and car model were combined to run the crash simulation. The initial car speed was set to 100 km/h with an impact angle of 20°. Contact definitions were established between the vehicle and the barrier, and among the barrier parts themselves. Since this is a dynamic test, the analysis was run in explicit mode. Before the run, many simulation parameters, such as termination time and plot time intervals, were defined in the model. The ASCII card was used to record test outputs, including displacements, velocities, and accelerations. General views of the initial condition of the real full-scale TB11 crash test and the FE model are provided in Figure 3.

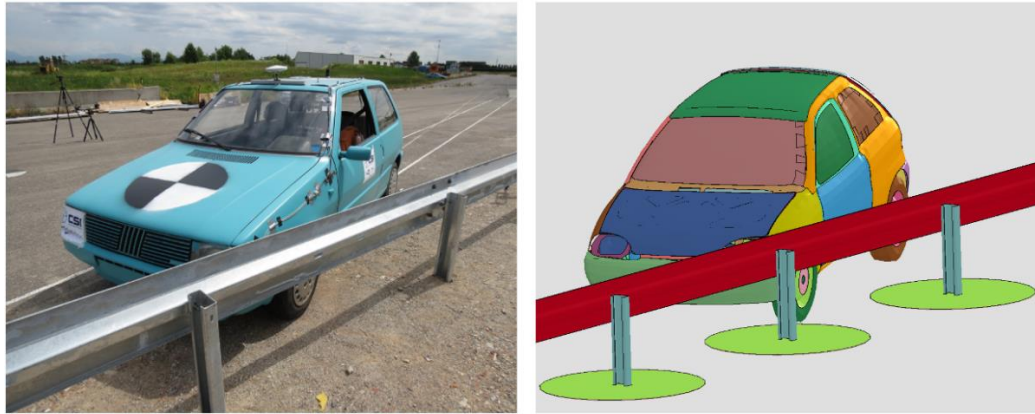


**Figure 3.** General View of H1 Barrier TB11 Test Before Test: Actual Test (left) (CSI, 2014), FE Simulation (right)

The actual full-scale crash test and computer simulation results were obtained and compared. The results and EN 16303 tolerances for the validation of virtual crash tests are summarized in Table 4. In the real TB11 test, ASI and THIV parameters were obtained as 0.68 and 20.86 km/h, respectively. According to these results, the impact severity level of this barrier is A, and the THIV result is within the EN 1317 acceptable limit. The working width was measured as 0.8 m, which corresponds to the W2 class. In the LS-DYNA simulation, on the other hand, ASI was obtained as 0.71, which is class A. THIV value was obtained as 22.5 km/h. The working width was determined as 0.77 m (W2). Results indicate that the actual crash test and simulation results are very close to each other, with variations within the specification limits. Both tests met the exit box and exit angle criteria described in EN1317-2. The relative differences between test outputs were lower than 10%. This level of deviation is acceptable for the validation of the FE model (Teng et al., 2015). In addition to these parameters, the ASI graphs of the real crash test and FE analysis are compared in Figure 4 (CSI, 2014). This graph shows the change in the ASI index over time, and there is good agreement between the curves obtained in the real test and simulation.

**Table 4.** Comparison of Barrier Performance Parameters Obtained from Real Test and Simulation.

Parameter	EN 16303 tolerance	Real crash test	FE model	Difference relative (%)
ASI	±0.1	0.68	0.71	4.4
THIV (km/h)	±3	20.86	22.5	7.9
W (m)	±0.1	0.8	0.77	3.8
Working width class	-	W2	W2	-

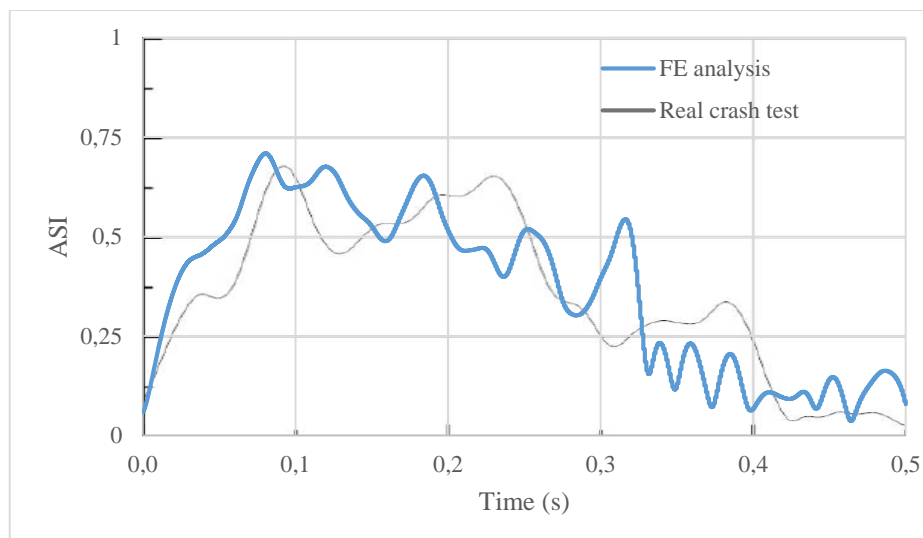


**Figure 4.** Comparison of ASI Graphs of Real Test (CSI, 2014) and Computer Simulation

The sequential picture comparison of the actual crash test and the FE model is provided in Figure 5. The impact angle and velocity were 20° and 100 km/h, respectively. The impact point was around the 10<sup>th</sup> post in the real test. During

the impact, posts 10-14 were detached from the rail due to the fracture of M10 connection bolts between the rail and post components. This controlled failure ensures the containment and redirection of the cars. The vehicle was contained by the barrier and redirected towards the roadside in accordance with EN 1317-2.

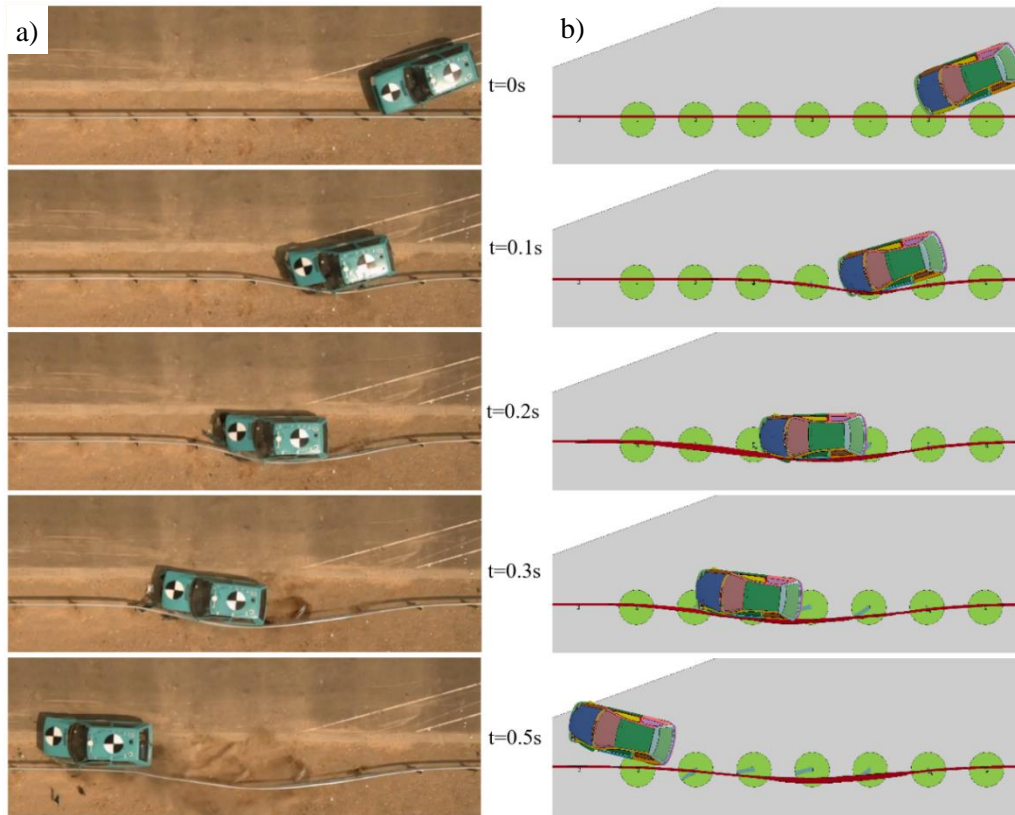


**Figure 5.** Comparison of TB11 Tests: **a)** Real Crash Test (left) (CSI, 2014), **b)** FE Simulation (right)

The barrier deformations occurring after the real crash test and FE analysis are depicted in Figure 6. Results indicate a very good agreement between FE simulation and real crash test results. Validation results confirm that the FE model could be used for further analyses in this research.

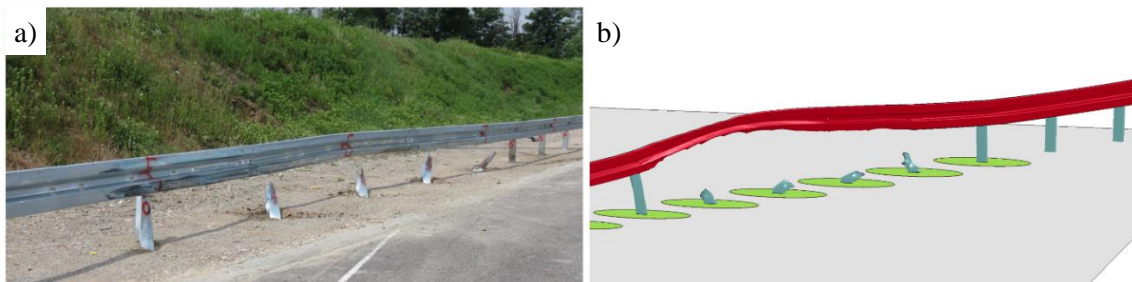


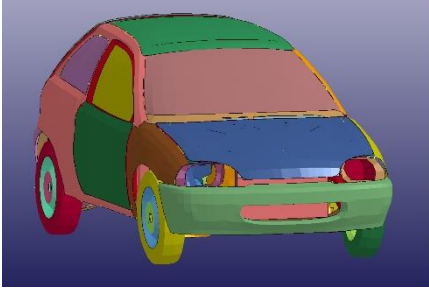
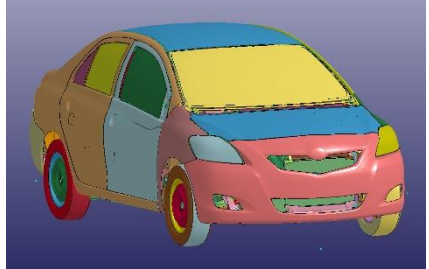
**Figure 6.** Deformation Comparison for H1 Barrier: **a)** After Real Test (CSI, 2014), **b)** FE Simulation

### ***Car FE Models Used in This Study***

To evaluate the impacts of electric cars on the crash performance of longitudinal barriers, three existing and verified car FE models were utilized. These previously validated car models were obtained from available LS-DYNA vehicle model libraries (CCSA, 2023; NCAC, 2008; NHTSA, 2023). These three models have different weights and dimensions. Before the simulations, the weights of all car FE models were adjusted to be within  $900 \pm 25$  kg. This ensured compliance with the vehicle mass requirement of the EN 1317 TB11 test. To simulate the crash performance of electric cars, reference electric car models were selected for each existing FE model, and the models were modified according to the properties of the reference cars. Electric vehicles were simulated by modifying the weights and centers of gravity (CG) of the existing car FE models. For the modification of the FE models, the Mass trimming interface (MassTr) within the LS-PrePost software was employed. Reference cars were selected to be as similar in dimensions as possible to the existing car models (Hyundai, 2023; MG, 2023; Renault, 2023).

Existing car FE models and reference cars used for electric car analyses are listed in Table 5. In addition to the TB11 simulations implemented for existing models, simulations were conducted again with vehicle FE models modified according to the reference electric vehicle properties. A total of six FE analyses, three for 900 kg vehicles and three for the modified models for electric cars were carried out.

**Table 5.** Existing FE Models and Reference Electric Cars

	Existing FE model		Reference electric car
Fiat-Uno (NCAC, 2008)		Renault Zoe (Renault, 2023)	
Toyota- Yaris (CCSA, 2023)		MG MG4 EV (MG, 2023)	
Dodge- Neon (NHTSA, 2023)		Hyundai Ioniq (Hyundai, 2023)	

Basic properties of the existing FE models, the reference electric cars, and the parameters used for the modification of the FE models are presented in Table 6. As shown in the table, the dimensions of the existing FE models and the selected reference cars are fairly similar. The first existing FE model was a Fiat-Uno brand car (Model-1). A Renault Zoe brand electric car was selected as a reference to modify the existing model. The properties of reference electric cars were obtained from the producer's webpage and other online sources (Autozine, 2023a; Renault, 2023). To simulate the behavior of the electric car, the mass and center of gravity (CG) height of the FE model were adjusted. The mass of the vehicle FE model was increased to 1502 kg. Compared to the initial model, the modified model is 602 kg heavier, and its center of gravity height is 35 mm lower. All other geometric dimensions of the model were kept the same as the initial model.

The second FE model was a Toyota-Yaris brand car (Model-2). To modify this model, an MG MG4 EV brand electric car was selected as a reference (MG, 2023). The dimensions of the reference EV were close to the existing FE model. The FE model was modified by changing its CG height and mass according to the EV properties. The FE model mass increased to 1655 kg. Compared to the initial model, the modified model is 769 kg heavier and its center of gravity height is 59 mm lower.

The third FE model was a Dodge-Neon brand car (Model-3). A Hyundai Ioniq brand car was used as a reference to modify the FE model (Hyundai, 2023). The geometric dimensions of the FE model were kept the same, and its mass and CG height were modified. Although information regarding the height of the CG of the Hyundai Ioniq brand car could not be found, since the center of gravity is 90 mm lower than the gasoline version of the electric vehicle with similar geometric dimensions, the model has been modified to have a 90 mm lower center of gravity (Autozine,

2023b). The mass of the vehicle FE model was increased to 1475 kg. Compared to the initial model, the modified model is 575 kg heavier, and its center of gravity height is 90 mm lower.

**Table 6.** Properties of Vehicle FE Models and Selected Reference Cars for EV Modification

		Brand	Height/ Width/ Length (mm)	Mass (kg)	CG height (mm)	Wheelbase (mm)	Wheel track (front/rear) (mm)
Model-1	Existing FE model	Fiat-Uno	1420/1580/3750	897	503.6	2376	1350/1370
	Reference Electric car	Renault Zoe	1562/1730/4087	1502	468.6	2588	1506-1489
	Modified FE model	Modified for Renault Zoe	1420/1580/3750	1502	468.6	2376	1350/1370
Model-2	Existing FE model	Toyota-Yaris	1465/1695/4300	886	549	2538	1490/1470
	Reference Electric car	MG MG4 EV	1504/1836/4287	1655	490	2705	1552/1562
	Modified FE model	Modified for MG MG4 EV	1465/1695/4300	1655	490	2538	1490/1470
Model-3	Existing FE model	Dodge-Neon	1370/1710/4355	900	510	2648	1450/1450
	Reference Electric car	Hyundai Ioniq	1450/1820/4470	1420-1575	-	2700	1552/1564
	Modified FE model	Modified for Hyundai Ioniq	1370/1710/4355	1475	420	2648	1450/1450

## RESULTS AND DISCUSSION

In this study, the effects of electric cars on the performance of the H1 containment level longitudinal safety barrier were investigated using explicit finite element software LS-DYNA. Computer simulations were performed using validated finite element models. Three different existing car models were utilized to conduct EN 1317 TB11 tests, which require a 900 kg car weight, 20° impact angle, and a 100 km/h impact speed. These car models were then modified using reference common EV models to represent the electric cars with heavier weights and lower center of gravity heights. To assess the effects of EVs, the performance of the barrier against existing 900 kg car models and modified models for reference EVs was evaluated. Injury severity of passengers was assessed using the ASI and THIV indices. The structural performance of the barrier was evaluated using the working width result and the final condition of the steel barrier. The calculated parameters and corresponding classes of all six tests are summarized in Table 7.

The results of the FE analyses performed using the first vehicle model (Model-1), where the vehicle weight was set to 900 kg for the TB11 test and 1502 kg to represent the Renault Zoe EV, are presented in the first column. Using the second model (Model-2), a 900 kg car test and a 1655 kg vehicle test representing MG MG4 EV were conducted. Finally, the results of the 900 kg car test performed using Model-3 and a 1475 kg vehicle test representing the Hyundai Ioniq EV are provided.

**Table 7.** Comparison of Safety and Performance Parameters Obtained Using 900 kg Models and Modified Models for EVs

Parameter	Model-1		Model-2		Model-3	
	Fiat-Uno	Modified for Renault Zoe	Toyota-Yaris	Modified for MG MG4 EV	Dodge-Neon	Modified for Hyundai Ioniq
ASI	0.71	0.69	0.73	0.44	0.83	0.73
THIV (km/h)	22.5	22	27.2	14.6	19.8	17.9
Working width (m)	0.77	0.90	0.61	Failed	0.63	0.91
Class of working width	W2	W3	W2	-	W2	W3

The ASI and THIV indices were calculated as 0.71 and 22.5 km/h, respectively, for the 900 kg version of Model-1. These indices were obtained as 0.69 and 22 km/h for the EV version of Model-1, respectively. The results demonstrate that increasing weight and lowering the center of gravity decrease the impact severity of occupants, as expected. In both cases, the calculated indices are within the limits of EN 1317-2, and the impact severity class is A. In both analyses, the vehicle impact points were around the 10<sup>th</sup> post. During the 900 kg vehicle impact, posts 10-14 were separated from the rail. However, in the EV analysis, posts 10-16 were separated from the rail after the failure of the beam elements defined between the post and rail. The deformed region in the barrier in the EV test was much longer compared to what was observed in the 900 kg car test. Working widths were measured as the largest lateral distance between the front side of the barrier and the deformed barrier during the impact. Working widths of the 900 kg and EV versions of Model-1 tests were measured as 0.77 m and 0.90 m, respectively. These widths correspond to W2 and W3 classes, respectively. These results indicated that damage caused by the EV was much greater than the standard 900 kg car. To better understand the structural performance of the barrier and the vehicle behavior, a comparison of the 900 kg car and EV tests is provided in Figure 7. The total test duration was set to 0.5 s, and sequential pictures were provided for these tests.

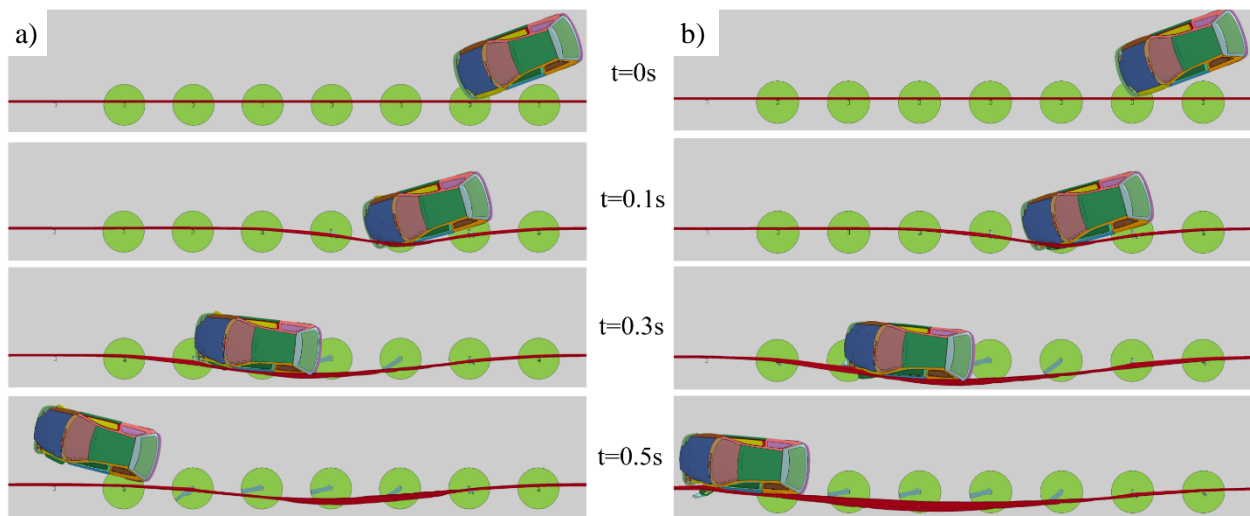


**Figure 7.** Comparison of 900 kg and EV Versions of Model-1 Crash Tests: **a)** 900 kg Car, **b)** EV Version

In the analyses performed with the 900 kg version of Model-2, the ASI and THIV indices were calculated as 0.73 and 27.2 km/h, respectively. In the analyses performed with the EV version weighing 1655 kg, these values were calculated as 0.44 and 14.6 km/h, respectively. Similar to the results of the Model-1, increased car weight and lower CG height reduced the impact severity of passengers. In both analyses, the impact points were around the 10<sup>th</sup> post. During the 900 kg vehicle impact, posts 10-15 were separated from the rail. The working width of the test barrier in the case of the 900 kg car impact was measured as 0.61 m, corresponding to W2 class. In the FE analysis of the H1 barrier with the EV model, the rail ruptured during the test and failed to contain the EV. The 86.8% increased impact energy (from 40 kJ to 74.7 kJ) due to the heavier vehicle caused this failure. The rupture in the rail occurred at the connection of the 10<sup>th</sup> post with the rail. With the increased impact energy, the fractured bolt connection region prorogated, and the rail was completely ruptured. A comparison of the 900 kg and EV models' behavior during the impact is shown sequentially in Figure 8.

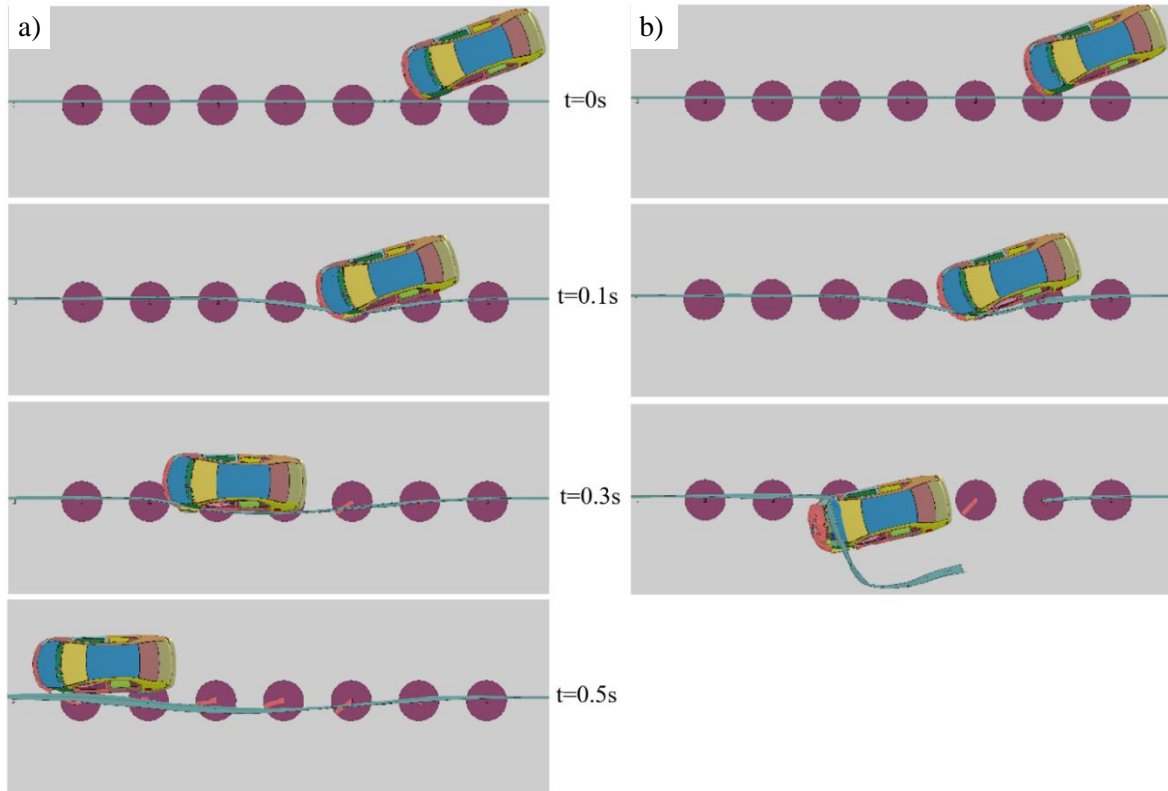


**Figure 8.** Comparison of 900 kg and EV Versions of Model-2 Crash Tests: **a)** 900 kg Car, **b)** EV Version

In the analyses performed with the 900 kg version of Model-3, the ASI and THIV indices were calculated as 0.83 and 19.8 km/h, respectively. In the analyses performed with the EV version weighing 1475 kg, these values were calculated as 0.73 and 19.9 km/h, respectively. Similar to the results of Model-1 and Model-2, increased car weight and lower CG height reduced the impact severity on occupants. In both analyses, the impact points were around the 10<sup>th</sup> post. During the 900 kg vehicle impact, posts 10-13 were separated from the rail. The damage in the barrier was less than in other two 900 kg car tests. The working width of the test barrier in the case of 900 kg car impact was measured as 0.63 m, corresponding to W2 class. In the FE analysis of the H1 barrier with the EV model, posts 11-16 were separated from the rail after the failure of the beam elements defined between the post and rail. The deformed region in the barrier in the EV test was much longer compared to what was observed in the 900 kg car test. The working width of the EV version of Model-3 was measured as 0.91, changing the working width class to W3. These results indicated that the damage caused by the EV was much greater than the standard 900 kg car. A comparison of the 900 kg and EV models' behavior during the impact is shown sequentially in Figure 9.

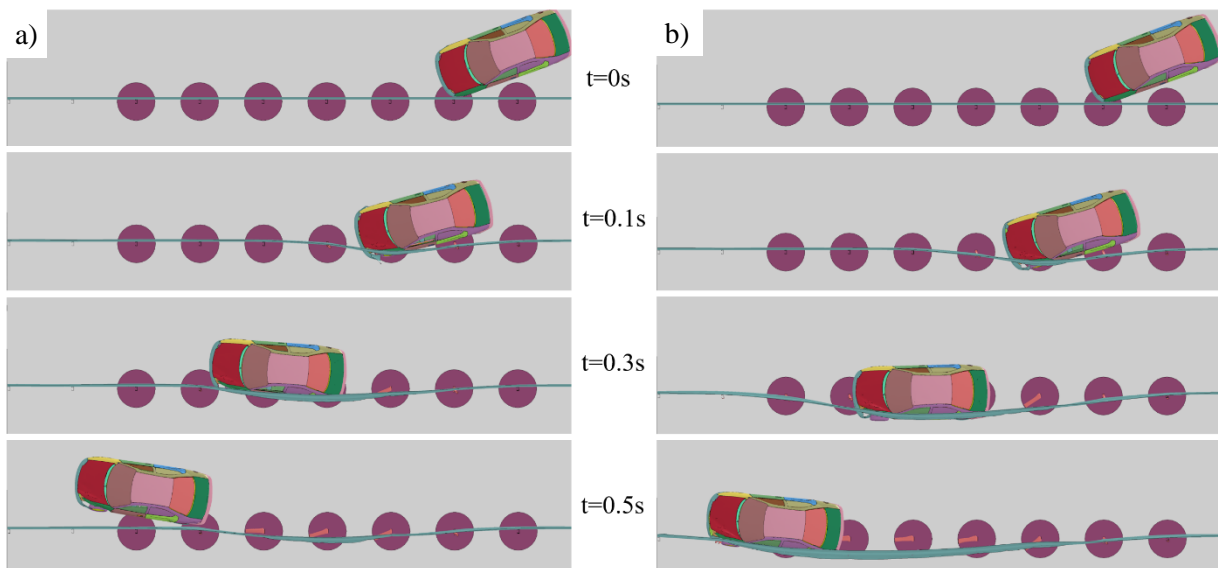


**Figure 9.** Comparison of 900 kg and EV Versions of Model-2 Crash Tests: **a)** 900 kg Car, **b)** EV Version

## CONCLUSION

In this study, the impact of electric cars on the performance of the H1 containment level steel longitudinal barrier was investigated. The finite element (FE) model of the barrier was validated using the results of a real full-scale TB11 test. A total of six FE analyses were conducted to assess the effect of electric cars with heavy weight and a low center of gravity on the impact severity and structural performance of the same longitudinal barrier. Computer simulations were performed with standard 900 kg internal combustion engine test vehicles and modified FE models representing three different reference electric cars. Subsequently, analyses results were evaluated. The main conclusions of this research study can be summarized as follows:

- Increasing vehicle weight decreased impact severity indices (ASI and THIV), reducing the risk of impact severity and improving injury protection for occupants.
- Analyses of Model-1 and Model-3 showed that electric cars significantly increased the working width and damaged region length of barriers. In the Model-2 analysis, a test failure occurred as a result of the rail breaking due to the increasing impact energy during the test with the electric car.
- Visual comparisons revealed that damage to vehicles and barriers was notably higher in tests conducted with electric car models.
- TB11 tests conducted with three different models of vehicles weighing 900 kg demonstrated that changing vehicle characteristics affected barrier performance. This emphasizes that even when the weight is the same, vehicle properties such as length, width, and CG height can influence test outcomes.

For future studies, it is recommended to conduct real full-scale crash tests to investigate the effects of electric vehicles on barrier performance. Therefore, modification of EN 1317 Part 2 to include electric vehicle option is recommended.

## REFERENCES

- AASHTO. (2016). *Manual for Assessing Safety Hardware* (Second Edition). American Association of State Highway and Transportation Officials (AASHTO).
- Atahan, A. O., Yücel, A. T., & Erdem, M. M. (2014). Crash testing and evaluation of a new generation L1 containment level guardrail. *Engineering Failure Analysis*, 38, 25-37. <https://doi.org/10.1016/j.engfailanal.2014.01.003>
- Atahan, A. O., & Yucel, A. O. (2013). Laboratory and field evaluation of recycled content sign posts. *Resources, Conservation and Recycling*, 73, 114–121. <https://doi.org/https://doi.org/10.1016/j.resconrec.2013.02.002>
- Atahan, A. O., Yucel, A. O., & Guven, O. (2013). Development of N2–H1 Performance-Level Guardrail: Crash Testing and Simulation. *Transportation Research Circular, E-C172*.
- Autozine. CG location of Renault (2023a). <http://www.autozine.org/Archive/Renault/new/Zoe.html> Accessed 15.10.23.
- Autozine. Renault Megane E-Tech Electric (2023b). [https://www.autozine.org/Archive/Renault/new/Megane\\_Electric.html](https://www.autozine.org/Archive/Renault/new/Megane_Electric.html) Accessed 01.11.23.
- Borovinšek, M., Vesenjāk, M., Ulbin, M., & Ren, Z. (2007). Simulation of crash tests for high containment levels of road safety barriers. *Engineering Failure Analysis*, 14(8), 1711–1718. <https://doi.org/https://doi.org/10.1016/j.engfailanal.2006.11.068>
- BS EN 16303:2020. (2020). Road restraint systems - Validation and verification process for the use of virtual testing in crash testing against vehicle restraint system. *BSI Standards Publication* .
- CCSA. Center for Collision Safety and Analysis, Finite Element models (2023). <https://www.ccsa.gmu.edu/models/> Accessed 15.10.23.
- CSI. (2014). *TB11 Test Report, H1 class Monolateral barrier for installation on soil*, CSI-SPA, Ballote, Italy.
- EN 1317-1. (2010). *Road restraint systems, Part 1: Terminology and General Criteria For Test Methods*. European Committee for Standardization: Brussels, Belgium.

- EN 1317-2. (2010). *Road restraint systems, Part 2: Performance classes, impact test acceptance criteria and test methods for safety barriers including vehicle parapets*. European Committee for Standardization: Brussels, Belgium.
- Gheres, M. I., & Scurtu, I. L. (2022). Crash testing and evaluation of W-beam guardrail using finite elements method. *IOP Conference Series: Materials Science and Engineering*, 1220(1), 012049. <https://doi.org/10.1088/1757-899X/1220/1/012049>
- He, L., & Lin, X. (2018). An improved mathematical model for vehicle crash against highway guardrails. *Archives of Transport*, 48(4), 41–49.
- Hyundai. Car specifications (2023). <https://www.hyundai.com/worldwide/en/eco/ioniq-electric/design> Accessed 15.10.23.
- IEA. Global EV Outlook 2023 (2023). <https://www.iea.org/reports/global-ev-outlook-2023> Accessed 13.11.23.
- Kim, K.-D., Ko, M.-G., Kim, D.-S., Joo, J.-W., & Jang, D.-Y. (2016). Strategy to increase the speed of a small car impact to a semi-rigid barrier designed for high impact severity. *International Journal of Crashworthiness*, 21(4), 310–322. <https://doi.org/10.1080/13588265.2016.1175052>
- Langseth, M., Hopperstad, O. S., & Berstad, T. (1999). Crashworthiness of aluminium extrusions: validation of numerical simulation, effect of mass ratio and impact velocity. *International Journal of Impact Engineering*, 22(9), 829–854. [https://doi.org/https://doi.org/10.1016/S0734-743X\(98\)00070-0](https://doi.org/https://doi.org/10.1016/S0734-743X(98)00070-0)
- LSTC. (2012). *LS-DYNA Keyword User's Manual*. Livermore Software Technology Corporation: Livermore, CA, USA.
- MG. Car specification (2023). <https://www.mg.co.uk/new-cars/mg4-ev> Accessed 15.10.23.
- Molan, A. M., & Ksaibati, K. (2021). Impact of side traffic barrier features on the severity of run-off-road crashes involving horizontal curves on non-interstate roads. *International Journal of Transportation Science and Technology*, 10(3), 245–253. <https://doi.org/https://doi.org/10.1016/j.ijtst.2020.07.006>
- Molan, A. M., Moomen, M., & Ksaibati, K. (2019). Investigating the effect of geometric dimensions of median traffic barriers on crashes: Crash analysis of interstate roads in Wyoming using actual crash datasets. *Journal of Safety Research*, 71, 163–171.
- NCAC. Finite element model archive, FHWA/NHTSA National Crash Analysis Center, George Washington University (2008). <http://www.ncac.gwu.edu/vml/models.html> Accessed 01.04.08.
- NHTSA. National Highway Traffic Safety Administration, Crash Simulation Vehicle Models (2023). <https://www.nhtsa.gov/crash-simulation-vehicle-models> Accessed 15.10.23.
- Özcanan, S., & Özcan, Ö. (2022). Criteria inadequacy of the vehicles used for the calculation of safety parameters in the EN1317-TB11 test. *Proceedings of the Institution of Mechanical Engineers, Part D: Journal of Automobile Engineering*, 237(4), 680–690. <https://doi.org/10.1177/09544070221115010>
- Ozcanan, S., & Atahan, A. O. (2021). Minimization of Accident Severity Index in concrete barrier designs using an ensemble of radial basis function metamodel-based optimization. *Optimization and Engineering*, 22(1), 485–519. <https://doi.org/10.1007/s11081-020-09522-x>
- Pawlak, M. (2016). The Acceleration Severity Index in the impact of a vehicle against permanent road equipment support structures. *Mechanics Research Communications*, 77, 21–28. <https://doi.org/https://doi.org/10.1016/j.mechrescom.2016.08.005>
- Reichert, R., Marzougui, D., & Kan, C.-D. (2020). *Crash Simulations Between Non-Occupied Automated Driving Systems and Roadside Hardware*. United States. Department of Transportation. National Highway Traffic Safety ....
- Ren, Z., & Vesenjaj, M. (2005). Computational and experimental crash analysis of the road safety barrier. *Engineering Failure Analysis*, 12(6), 963–973. <https://doi.org/https://doi.org/10.1016/j.engfailanal.2004.12.033>
- Renault. Car specifications (2023). <https://www.renault.co.uk/electric-vehicles/zoe/specifications.html> Accessed 15.10.23.
- Teng, T.-L., Liang, C.-C., Hsu, C.-Y., Shih, C.-J., & Tran, T.-T. (2016). Impact performance of W-beam guardrail supported by different shaped posts. *International Journal of Mechanical Engineering and Applications*, 4(2), 59–64.

Teng, T.-L., Liang, C.-C., & Tran, T.-T. (2015). Effect of various W-beam guardrail post spacings and rail heights on safety performance. *Advances in Mechanical Engineering*, 7(11), 1687814015615544. <https://doi.org/10.1177/1687814015615544>

Wolny, R., Bruski, D., Budzyński, M., Pachocki, L., & Wilde, K. (2022). Influence of a Lighting Column in the Working Width of a W-Beam Barrier on TB51 Crash Test. *Materials*, 15(14). <https://doi.org/10.3390/ma15144926>

Yücel, A. Ö., Atahan, A. O., Arslan, T., & Sevim, U. K. (2018). Traffic Safety at Median Ditches: Steel vs. Concrete Barrier Performance Comparison Using Computer Simulation. *Safety*, 4(4). <https://doi.org/10.3390/safety4040050>